Azo-carbazole dye chromophore as promising materials for diffraction grating recording

ARTICLE *in* JOURNAL OF MATERIALS SCIENCE MATERIALS IN ELECTRONICS · OCTOBER 2010

Impact Factor: 1.57 · DOI: 10.1007/s10854-009-0039-5

3 AUTHORS, INCLUDING:

Jacek Niziol

AGH University of Science and Technology i…

85 PUBLICATIONS **327** CITATIONS

J Mater Sci: Mater Electron (2012) 23:2194–2201
DOI 10.1007/s10854-012-0749-y

Characterization of solution and solid state properties of polyaniline processed from trifluoroacetic acid

J. Nizioł · Ewa Gondek · K. J. Plucinski

Received: 17 March 2012 / Accepted: 2 May 2012 / Published online: 11 May 2012

Abstract In this work are reported properties of polyaniline processed from trifluoroacetic acid. Films obtained by simple drop casting were smooth and defectless. Features like absorption in range of UV–vis-NIR, mid-IR and electrical conductivity are discussed. The highest electrical conductivity of such films was found equal to 65 S/cm. It was observed a striking feature—successive colour transition from cyan to deep green when the solvent was dried out from the cast film.

1 Introduction

Polyaniline (PANI) for the last three decades has been a one of the most intensively investigated conjugated polymers, because of its intrinsic electrical conductivity, simple and cheap production. The most widely employed method of polyaniline synthesis involves chemical oxidation in an acidic environment. A rage of oxidizing agents is currently available [1]. It is an easy process, delivering bulk quantities of the polymer and thus superior to competitive techniques. Properties of the final product can be easily tailored. Small quantities of good quality PANI can be obtained through electrochemical polymerization [2]. Some less exploited polymerization techniques are plasma polymerization [3] or solid-state polymerization [4].

Polyaniline may exist in a variety of forms, which differ one from other by the ratio of phenylene amine to quinone imine units. The form consisting of equal number of both units is designated emeraldine. From chemical point of view this polymer is a base [emeraldine base (EB)]. It is electrically insulating, but simple protonation boosts it to conducting state. The protonation creates polarons [5], charge carriers able to travel along the macromolecule backbone or even to move on neighbouring macromolecules through variable range hopping (VRH) mechanism [6]. In effect the electrical conductivity may be enhanced by as much as ten ranges of order. Because of chemistry, the conducting form of polyaniline is called emeraldine salt [7] (ES). The structure of both forms of emeraldine is shown in Fig. 1. The protonating agent is colloquially referred to as "dopant" and the all over process to as "doping". Theoretically the highest conductivity is achieved when each imine nitrogen is protonated, in other words at the doping level $y = 0.5$.

Intrinsically conducting polymers in general, and polyaniline in particular are difficult to process, because they do not melt at temperatures below decomposition. Since late 80-ties of the last century a lot of effort has been done to resolve the problem of PANI intractability. Many authors confirmed strong polar and hydrogen-bonding interactions in different forms of polyaniline [8]. This feature explained lack (or very poor) solubility of this polymer in the majority of common solvents and tendency to precipitate from already made solutions. Therefore, solubilization strategy must involve solvents providing competitive chain-solvent interactions. Films cast from EB solution in non-protonating liquids were not conductive and required post-doping, what

J. Nizioł
Faculty of Physics and Applied Computer Science, AGH University of Science and Technology, al. Mickiewicza 30, 30-059 Krakow, Poland

E. Gondek
Institute of Physics, Cracow University of Technology, Podchorążych 1, 30-084 Krakow, Poland

E. Gondek · K. J. Plucinski (✉)
Electronics Department, Military University Technology, 00-908 Warsaw, Poland
e-mail: kpluc2006@wp.pl

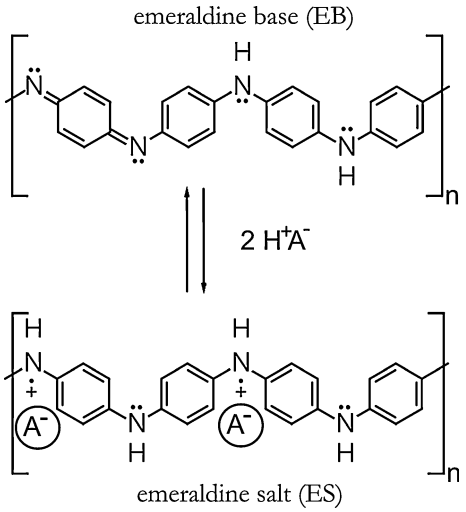

Fig. 1 Scheme of emeraldine protonation (adapted from [38])

rarely led to homogenous conductivity. For this reason it is more convenient to prepare three component solution containing EB, the dopant and the solvent. Working example of such strategy was for the first time reported in [9] where good quality conductive films (up to 300 S/cm) were obtained from m-cresol solution of EB and camphorsulfonic acid (CSA). To date, improvements extended electrical conductivity of such films to 1,300 S/cm [10], in addition manifesting truly metallic character. However, it is virtually impossible to completely remove m-cresol after casting, because it plays role of so-called secondary dopant [11]. The deposited layers tend to release slowly the solvent over a prolonged time, what constitutes their significant drawback. The poor PANI solubility can be also circumvented by its preparation in form of water dispersion [12], doping with compounds bearing plasticizing moieties [13] or polymerisation of aniline derivatives (such as ortho-toluidine) [14]. This approach renders polyaniline compatible to popular solvents, but usually decreases the electrical conductivity.

Remarkable electronic, optical and redox properties make polyaniline attractive for a number of practical applications such as corrosion protectors [15], gas sensors [16], biosensors [17], Schottky diodes [18], organic light emitting devices [19] or photovoltaic cells [20]. PANI deposited in form of a thin layer is a common component of all these devices. Usually such layers are fabricated by casting, dip-coating, Dr.Blade method or spin-coating from solution. To formulate solution well suited to such proceeding, one should use an easily evaporating solvent of low surface tension and viscosity. The last feature ensures smooth distribution of the solution over the substrate. Important data, collected from available handbooks and encyclopaedias, illustrating properties of routinely used solvents of polyaniline are tabulated in Table 1. So far, the last cited solvent, trifluoroacetic acid (TFA) was little unexploited in polyaniline treatment [21, 22]. It represents particularly low surface tension and viscosity comparing to competitors. Trifluoroacetic acid has also low boiling temperature and vapour pressure, what assures rapid solvent removal. These facts suggested usefulness of TFA for processing good quality thin films of polyaniline, what was verified in frame of the current work.

2 Experimental section

2.1 Methods and instruments

The instruments used for properties characterization were CHN S/O 2400 Perkin Elmer (elemental analysis), Lambda 9000 Perkin Elmer (UV–vis-NIR spectroscopy), Biorad FTS-6000 (FTIR spectroscopy), an arrangements consisting of Keithley 487 picoammeter, Keithley 2400

Table 1 Properties of some of the most popular polyanilne solvents

	Solvent	T_m [°C]	T_b [°C]	S_t [mN/m] (at 25 °C)	V_s [mPa·s] (at 25 °C)	V_p (kPa)	pKa	μ [D]	Ref.
1	NMP n-methylpyrrolidone	24	202	41.00	1.7	0.039	–	4.06	[33]
2	DMF Dimethylformamide	−60.5	153	n/a	0.794	0.439	–	3.86	[5]
3	DMSO dimethyl sulfoxide	17.9	189	42.92	1.987	0.084	–	3.96	[34]
4	*Metha*-cresol	12.2	202.3	35.69	12.9	0.019	10.09	1.48	[1]
5	Formic acid	8.3	101	37.13	1.607	5.75	3.75	1.43	[35]
6	Chloroform	−63.4	61.2	26.67	0.537	26.2	≈24	1.04	[33]
7	Dichloroacetic acid	13.5	194	35.40	n/a	n/a	1.35	n/a	[36]
8	HFIP hexafluoro-2-propanol	−3.3	58.2	16.14	1.65	26.9 (30 °C)	9.3	n/a	[37]
9	TFA trifluoroacetic acid	−15.4	72.4	13.53	0.808	15.1	0.52	2.28	–

T_m Melting point, T_b boiling point, S_t surface tension, V_s viscosity, V_p vapour pressure, pK_a acidity constant, μ electric dipole moment, *Ref.* reference reporting the given solvent (1–8) used to dissolve polyaniline

Table 2 Results of elemental analysis

			C [%]	H [%]	N [%]	S [%]	F [%]	O (to 100 %)
1	PANI/TFA	Found	53.58	3.49	9.03	–	18.97	14.93
		Theoretical	53.93	3.67	8.92	–	19.22	14.36
2	PANI-CSA/ TFA	Found	55.83	5.81	5.52	7.17	5.44	20.23
		Theoretical	56.42	5.73	5.41	7.03	5.39	20.06

Fitted formulas

(1) PANI/TFA $(PANI)_1(TFAA)_{0.53}(H_2O)_{0.35}$

(2) PANI-CSA/TFA $(PANI)_1(TFAA)_{0.25}(CSA)_{0.51}(H_2O)_{0.48}$

$PANI_1$ stands for repeating unit containing benzenoid ring

source-meter and Advanced Research Systems DE-202 cryostat (electrical measurements).

2.2 Materials and samples

Aniline was freshly synthesised by POCh (Poland) and used without further purification. All other chemicals were purchased from Aldrich and used as received. The initial PANI-HCl powder was synthesised by oxidative radical polymerization of aniline in aqueous solution, [1]. The monomer solution contained 150 ml (1.62 mol) of aniline, 1500 ml of 2 M hydrochloric acid and 50 g (1.17 mol) of lithium chloride, oxidizing solution consisted of 94 g (0.41 mol) of ammonium persulfate in 1,000 ml of 2 M HCl. The polymerization was carried out at stabilized temperature in the vicinity of 0 °C. All solutions were cooled to this temperature before the reaction started. The oxidizer was added dropwise to vigorously stirred monomer solution for 15 min at a rate avoiding the sudden rise of the temperature. The last is typical for the standard procedure and results in poorer quality of the synthesised product. After 2 h the reducing solution (60 g of $FeCl_2$ in 1,000 ml of 2 M HCl) was added in a single shot to stop the reaction. The precipitate was collected in a large Buchner funnel and rinsed with 1 M HCl and next with deionised water until neutral pH. This greenish product was immersed and agitated in abundance of 0.1 aqueous ammonia for 24 h. Filtered off, it was consecutively washed with methyl alcohol then ethyl ether, each time until the wash solution was colourless. After that, the product was dried under dynamic vacuum to constant mass. The obtained dark navy blue powder was supposed to be polyaniline in oxidation state of emeraldine base.

The stock solutions were prepared by putting EB in TFA, and in TFA with previously dissolved CSA in a stoichiometry assuring theoretical doping level $y = 0.5$. These solutions will be further referred to as PANI/TFA and PANI-CSA/TFA. They were mechanically stirred within 24 h. The kinetics of dissolving depended on different factors, like ratio of solutes to the solvent, stirring speed, temperature volume of the vessel etc. PANI-CSA/TFA became a smooth, opaque liquid without visible (in optical microscope scale) particulates, thus believed being a true solution. PANI alone, although partially soluble, dissolved much worse. Most of the polymer remained in solid state. In contrast for example to solutions prepared in m-cresol, PANI-CSA/TFAA didn't undergo jellification even after 2 years storage in ambient conditions. Complete dissolving can be reduced to minutes by adding a common plasticizer. In our case it was diethyl phtalate (0.1 molecule for one PANI ring-unit). Same procedure employing regular acetic acid as the solvent didn't work at all, even if much larger quantity of the plasticizer was added. This fact evidences crucial role played by fluorination of the solvent. However, as it was further checked, the electrical conductivity of samples prepared from the plasticized solution was lower by about one range of order. For this reason additional extra plasticizing procedure was abandoned. Thin solid films were proceeded from solutions by drop casting on quartz glass substrates or KBr pellets. At first samples were kept under a laboratory hood, then transferred (after about 15 min, when sample became visibly dry) to a vacuum drier and conditioned there at 80 °C until constant mass (24 h). Reference solutions and films of PANI-CSA ($y = 0.5$) in solvents cited in the Table 2, were prepared in a similar way.

3 Results and discussion

The synthesised polymer was identified as emeraldine base by elemental analysis (calculated/found %C: 79.55/78.75, %H 5.01/5.11, %N: 15.44/15.28) and FT-IR spectroscopy (Fig. 3). The bands at 1,508 and 1,594 cm^{-1} were assigned to benzene and quinoid ring, 1,322 cm^{-1} to C–N secondary amine asymmetrical stretching, 1,164 cm^{-1} to N=Q=N stretching (Q-quinone ring) and 836 cm^{-1} to C–H out-of-plane in substituted benzenoid ring [26]. The reduced viscosity of 0.1 %wt. solution in 96 % sulphuric acid is often used as indicator molecular mass of polyaniline. In

the case of the synthesised EB, this parameter was equal to 1.2 dl/g, what allows to situate the molecular mass somewhere between 20,000 and 60,000 [23]. The electrical conductivity of EB powder compressed into pellet was in the range of 10^{-10} S/cm.

Experimental data obtained in result of elemental analysis of PANI-CSA/TFA film and solid state residues of PANI/TFA are given in Table 2. They were fitted with models assuming polyaniline, CSA, solvent and residual water content in the studied samples. The best matching formulas to theoretical predictions are set out in the last row of Table 2. As can be seen there, one ring repeating unit of polyaniline was accompanied by 0.53 molecule of TFA in the material obtained from PANI/TFA. This value corresponds to ideal doping. Pellets manufactured from such powder had their electrical conductivity in the range of 2 S/cm, what is typically reported for classical PANI doped with hydrochloric acid. So it may be supposed that these samples were fully protonated with TFA. More mysterious case was that of PANI-CSA/TFA film. Each polyaniline unit was accompanied by 0.51 of CSA molecule and 0.25 of TFA molecule. Assuming PANI protonation with only a fraction of available CSA molecules, the rest of CSA should be present in a crystalline form. Such situation often happens in polymeric systems containing a non bound molecular phase. However characteristic sharp intense lines of CSA crystallites were not observed in X-ray diffraction spectrum. Thus, as a possible explanation may serve hydrogen bonds between TFA molecules and carbonyl moieties of CSA like it happens in the case of PANI-CSA cast from m-cresol [11].

The FT-IR spectrum of TFA was recorded using a KBr pellet previously incubated in saturated vapours of this solvent (Fig. 2). In this spectrum manifest vibrations at 1,676 cm^{-1} (C=O stretching) [24], at 1,436 cm^{-1} (in plane bending of COH), a range of peaks between 1,140 and

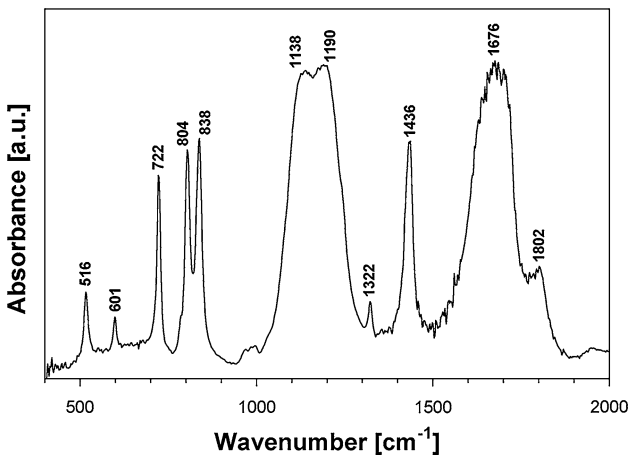

Fig. 2 FTIR spectrum of TFA

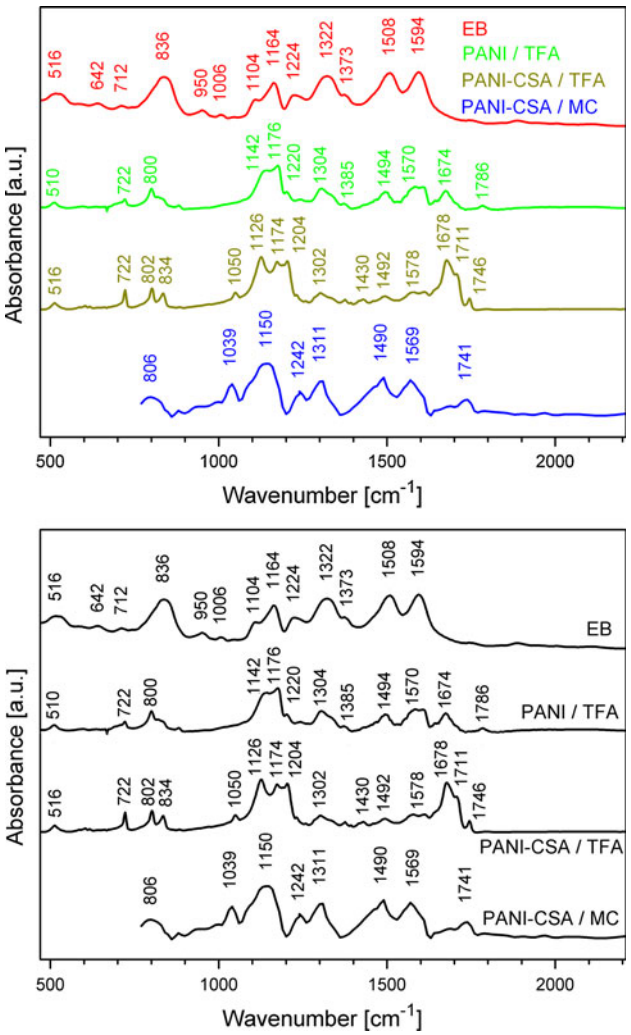

Fig. 3 FT-IR spectra (from *up* to *down*): synthesised EB (emeraldine base) in KBr pellet and cast on KBr pellet PANI from TFA, PANI-CSA from TFA, PANI-CSA from MC. (*colour figure* for on-line dissemination only)

1,320 cm^{-1} (attributed to vibrations of CF_3 [25]) and a series of characteristic sharp bands at 722, 804 and 834 cm^{-1}. FT-IR spectra of different PANI forms are shown in Fig. 3. Peaks issued from polyaniline may be seen at from 1,490 to 1,508 cm^{-1} (C=C stretching in benzenoid ring) and at from 1,578 to 1,594 cm^{-1} (C=C stretching in quinoid ring) [26]. Fingerprint band of CSA carbonyl moiety appears at the vicinity of 1,740 cm^{-1} [27]. Residual water is the origin of the peak at 1,608–1,612 cm^{-1} [27].

Comparative inspection of plots shown in Fig. 3 demonstrates that in the spectrum of PANI-CSA/TFA vibrations characteristic of pure TFA remain almost unchanged, while they are severely modified in the spectrum of PANI/TFA. The last proves more intense interactions between polyaniline and TFA molecules in absence of CSA. It should be also noticed a difference in ratio of 1,500 and 1,590 cm^{-1} peaks. In the case of EB and PANI-CSA/MC

film they are of similar height, while in spectra of TFA cast films the peak relative to quinoid ring vibration is more intense.

In the majority of available solvents conducting polyaniline adopts *compact-coil* conformation. In such a case, the morphology of UV–vis-NIR spectra features broad bands at c.a. 330 nm (attributed to π–π^* transition), at c.a. 400–450 nm (polaron-π^*) and at c.a. 750–800 nm (π-polaron) [28]. In the case of solvents promoting *expanded-coil* conformation in the spectrum appears also so-called free-carrier tail, rising towards the near infrared region [28] (a classical example is PANI-CSA/MC in Fig. 4. This feature is explained by a more regular and wider polaron band following polymer backbone conformation. In the solid state, it correlates with increasing electrical conductivity. Closer look at graphs in Fig. 4 doesn't reveal peaks at c.a. 600–650 nm (arising from n$-\pi$ transition and observed for emeraldine base). It means that in all solutions polyaniline was completely protonated. It can be also postulated that in PANI/TFA solution the polymer had compact-coil conformation and little more expanded in PANI-CSA/TFA, but less than in the case of PANI-CSA/MC solution. Since TFA is a strong acid, it was necessary to verify if it was in competition with CSA for protonation. A series of solution with different CSA content was prepared. As shown in Fig. 5, less extended free carrier tail appeared for doping level below the optimum value of 0.5 as well as in the case of important CSA excess. The last was expected, because non bound CSA ions cause electrical screening, facilitating "compact-coil" conformation of the polymer chain [29]. Thus, it may be assumed that CSA dominates PANI protonation if not monopolizes it entirely.

In controlled and reproducible conditions, the excess of TFA, owing to its volatility, evaporated from the cast films faster than any of reference solvents. FT-IR spectra measured for the same sample 20 min after casting in laboratory atmosphere and after 24-h conditioning in vacuum drier at 80 °C were identical. It proves that practically all non-bounded TFA evaporated prior to the treatment in the vacuum. Same experiment carried out on a reference sample from HFIP showed differences in the spectra, attributed to residual solvent, meanwhile released in the vacuum. In the case of m-cresol (high temperature boiling solvent) stable FT-IR spectrum required drying within days if not weeks.

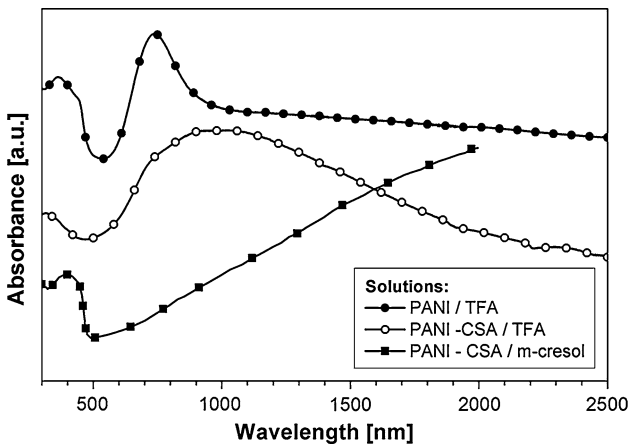

Fig. 4 UV–vis-NIR spectra of polyaniline solutions in TFAA

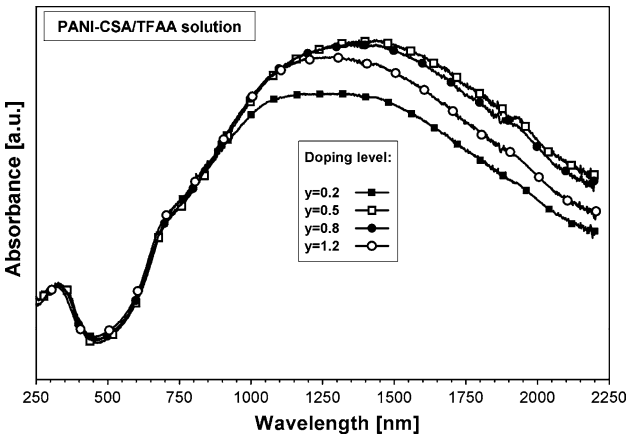

Fig. 5 UV–vis-NIR spectra of PANI-CSA/TFAA solutions of different doping levels

In UV–vis-NIR spectrum of drying PANI-CSA/TFA solution dried, the free carrier tail grew continuously. Spectroscopy data were transformed into colour coordinates, known also as CIE 1931 diagram. This illustrates colour variations in more comprehensive way, reproducing naked-eye observation. In Fig. 6 one can view colour of the sample, continuously changing from blue-cyan to deep green. This specific phenomenon may arise from reorganization of polymer conformation. The initial compact-coil form, forced by the excess of TFA, transforms to extended coil upon successive solvent evaporation. The colour change after casting was not observed in samples cast from HFIP, also fluorinated, but much less acidic solvent.

Another peculiarity was observed in the solid state. A series of films were prepared by casting same portions of consecutively diluted PANI-CSA/TFA stock solution, what provided decreasing thickness of resulted films. The extent of the free carrier tail in NIR absorption spectrum along with electrical conductivity were proportional to the sample thickness, as shown in Fig. 7. The threshold thickness for this phenomenon was about 1,000 nm. Similar dependencies, but not so strong were observed in the case of reference samples cast from HFIP. "Conductivity-friendly" conformation adopted by the polymer in the bulk in contrast to less conductive form present at the surface may account for this issue.

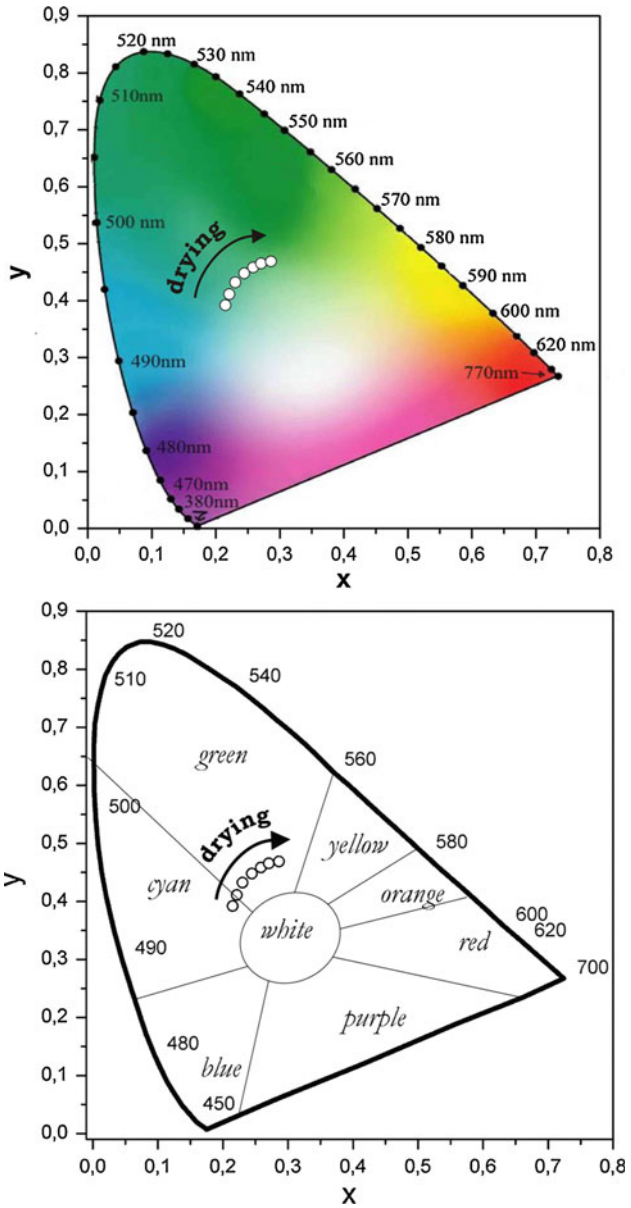

Fig. 6 Time dependence of UV–vis-NIR spectrum of a PANI-CSA/TFAA film (200 nm thick). Spectroscopy data were converted to coordinates of CIE (1931) xy chromaticity diagram. (*colour figure* for on-line dissemination only)

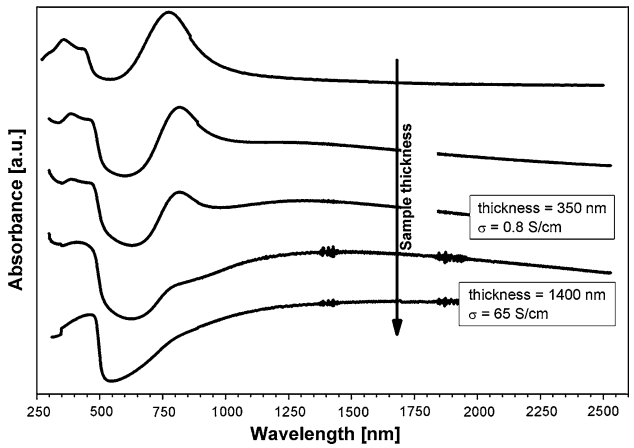

Fig. 7 UV–vis-NIR spectra and electrical conductivity dependence on thin film thickness. Because of technical constrains, only for two samples thickness and electrical conductivity were measured

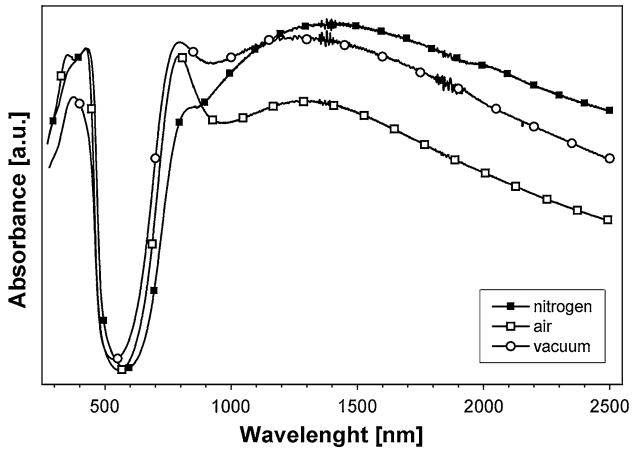

Fig. 8 UV–vis-NIR spectra changes of freshly prepared solid state film (300 nm thick), split into *three portions* and each stored in different atmospheres for 1 week

Optical spectra of films were sensitive to the conditioning atmosphere as illustrated in Fig. 8. The least developed free carrier tail was observed in the case of the sample stored in open air, what may be explained by humidity pick-up from the surrounding atmosphere. The humidity usually deteriorates electrical properties of polyaniline [30].

Results presented above let put forward assumption that the "doping power" of CSA is stronger than that of TFA, despite much higher accidity ($pK_a = 0.23$) of this later one.

Electrical conductivity measurements were carried out in cryogenic conditions in four contacts geometry. The applied test currents were as small as possible and the sample was in close contact with sapphire glass support to avoid heating through Joule effect. The sample thickness was c.a. 1,500 nm, thus in the range where the conductivity was thickness independent. In result of cooling down to temperature of 6 K, the conductivity dropped to about 3 % of its initial value. The graph plotted in terms of reduced activation energy versus temperature (not shown here), indicates that the system was just on insulating side of metal-insulator transition [31]. In such a case, the electrical conductivity is discussed within formalism of Mott's Variable Range Hopping (VRH) [32], considered valid up to temperatures between 200 and 300 K. It predicts temperature dependence of the conductivity by:

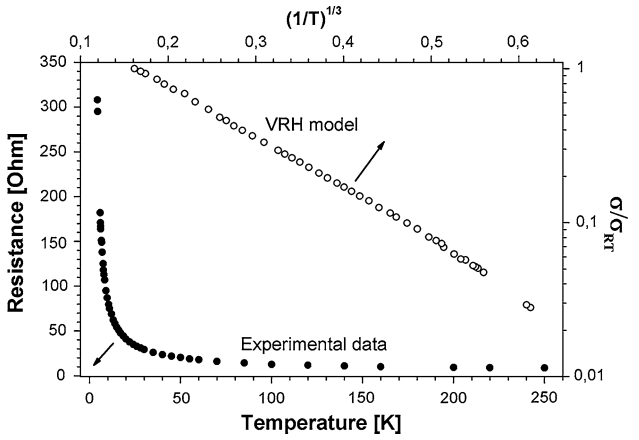

Fig. 9 Resistance versus temperature for PANI-CSA/TFAA film (*bottom-left*) and fit to VRH conductivity model (*top-right*), σ_{RT} conductivity at room temperature

$$\sigma(T) \simeq \sigma_0 \exp\left[-\left(\frac{T_0}{T}\right)^{\gamma}\right] \quad (1)$$

where σ_0 is the high temperature limit of conductivity, T_0 is characteristic temperature associated with the degree of localization of the wave function and the exponent is related to system dimensionality d as $\gamma = 1(d + 1)$. Plot of $\log(\sigma(T))$ versus T have to be linear within VRH model limits. Additional role here may play interaction with the vibrations which change effective mobilities of the carriers [39–41]. In the studied case the best fit was calculated applying $\gamma = 1/3$ as represented in Fig. 9. This value suggests two dimensional geometry of the system.

4 Conclusions

Trifluoroacetic acid is as an efficient solvent of conducting polyaniline for fabrication good quality thin films by simple drop casting. Drop casting is a more economic technique then spin-coating, typically employed for this purpose. The obtained films adhered much better to supports and their thickness was possible to be varied by diluting the stock solution. These issues make trifluoroacetic acid an interesting alternative to classical polyaniline solvents, at least in the case of selected applications. The observed particular optical properties were preliminary explained; however they need a more detailed study.

Acknowledgments The authors acknowledges partial financial support from polish Ministry of Science and Higher Education.

References

1. J. Niziol, M. Sniechowski, A. Podraza-Guba, J. Pielichowski, Polym. Bull. **66**, 761–770 (2011). doi:10.1007/s00289-010-0309-7
2. E.M. Genies, C. Tsintavis, J. Electroanal. Chem. **195**, 109–128 (1985)
3. G.J. Cruz, J. Morales, M.M. Castilio-Ortega, R. Olayo, Synth. Met. **88**, 213–218 (1997)
4. J.X. Huang, J.A. Moore, J.H. Acquaye, R.B. Kaner, Macromolecules **38**, 317–321 (2005)
5. M. Angelopoulos, G.E. Asturias, S.P. Ermer, E.M. Scherr, A.G. MacDiarmid, M. Akhtar, Z. Kiss, A.J. Epstein, Mol. Cryst. Liq. Cryst. **160**, 151–163 (1988)
6. R.P. McCall, J.M. Ginder, M.G. Roe, G.E. Asturias, E.M. Scherr, A.G. MacDiarmid, Phys. Rev. B **39**, 10174–10178 (1989)
7. D.C. Trivedi in *Handbook of organic conductive molecules and polymers*, vol 2, ed. by H.S. Nalwa (Wiley & Sons, New Jersy, 1997), p. 505
8. L.W. Shacklette, Synth. Met. **65**, 123–130 (1994)
9. Y. Cao, P. Smith, A.J. Heeger, Synth. Met. **48**, 91–97 (1992)
10. K. Lee, S. Cho, S.H. Park, A.J. Heeger, C.-W. Lee, S.-H. Lee, Nature **441**, 04705 (2006)
11. O.T. Ikkala, L.-O. Pietila, L. Ahjopalo, H. Osterholm, P.J. Passiniemi, J. Chem. Phys. **103**, 9855–9864 (1995)
12. J. Jang, J. Ha, J. Cho, Adv. Mater. **19**, 1772–1775 (2007)
13. T.E. Olinga, J. Fraysse, J.P. Travers, A. Dufresne, A. Pron, Macromolecules **33**, 2107–2113 (2000)
14. M. Leclerc, J. Guay, L.H. Dao, Macromolecules **22**, 649–653 (1989)
15. Wallace G.G., Spinks G.M., Kane-Maguire L.A.P., Teasdale P.R. *Conductive electroactive polymers*, (CRC Press, Boca Raton 2009), p. 22, ISBN 978-1-4200-6709-5
16. J. Gong, Y. Li, Y. Hu, Z. Zhou, Y.J. Deng, Phys. Chem. C **114**(21), 9970–9974 (2010)
17. H. Chang, Y. Yuan, N. Shi, Y. Guan, Anal. Chem. **79**(13), 5111–5115 (2007)
18. F. Yakuphanoglu, E. Basaran, B.F. Senkal, E. Sezer, J. Phys. Chem. B **110**(34), 16908–16913 (2006)
19. J. Jang, J. Ha, K. Kim, Thin Solid Films **516**(10), 3152–3156 (2008)
20. W. Wang, E.A. Schiff, Appl. Phys. Lett. **91**, 133504 (2007)
21. W. Łużny, E.J. Samuelsen, D.W. Breiby, Fibres Text. East. Eur. **11**(5), 97–100 (2003)
22. T.J. Kang, D.N. Kim, K.H.J. Hong, Appl. Polym. Sci. **124**, 4033–4037 (2012)
23. Cao Y., Smith P., Heeger A.J. in *Low-dimensonal systems and molecular electronics*, ed. by R.M. Metzger, P. Day, G.C. Papavassiliou, NATO ASI Series B: Physics, vol. 248, (Plenum Press, New York, 1991), p. 317
24. Keller J.W., J. Phys. Chem. A **108**, 4610–4618 (2004)
25. Bruno T.J., Svoronos P.D.N., CRC handbook of fundamental spectroscopic correlation charts, chapter 2, ISBN 0-8493-3250-8, (Taylor & Francis, London, 2006)
26. J. Laska, J. Widlarz, Polymer **46**, 1485–1495 (2005)
27. J. Stejskal, I. Sapurina, M. Trchova, J. Prokes, I. Krivka, E. Tobolkowa, Macromolecules **31**, 2218–2222 (1998)
28. Y. Xia, J.M. Wiesinger, A.G. MacDiarmid, A.J. Epstein, J. Chem. Mater. **7**, 443–445 (1995)
29. A.G. MacDiarmid, A.J. Epstein, Synth. Met. **65**, 103–116 (1994)
30. J.P. Travers, M. Nechtschein, Synth. Met. **21**, 135–141 (1987)
31. A. Ahlskog, M. Reghu, A.J. Heeger, J. Phys. Condens. Mater. **9**, 4145–4156 (1997)
32. N.F. Mott, *Metal-Insulator Transition*, 2nd edn. (Taylor and Francis, London, 1990), p. 50
33. Y.N. Xia, A.G. MacDiarmid, A.J. Epstein, Macromolecules **27**, 7212–7214 (1994)
34. M.Y. Hua, G.-W. Hwang, Y.-H. Chuang, S.-A. Chen, Macromolecules **33**, 6235–6238 (2000)
35. M. Zagorska, E. Taler, I. Kulszewicz-Bajer, A. Pron, J. Niziol, J. Appl. Phys. Sci. **73**, 1423–1426 (1999)

36. Y. Cao, J. Qiu, P. Smith, Synth. Met. **69**, 187–190 (1995)
37. P. Rannou, A. Gawilicka, D. Berner, A. Pron, M. Nechtschein, Macromolecules **31**, 3007–3015 (1998)
38. A.G. MacDiarmid, J.C. Chiang, A.F. Richter, Synth. Met. **76**, 285–288 (1988)
39. E. Gondek, I.V. Kityk, A. Danel, Philos. Mag. Lett. **89**, 807–819 (2009)
40. E. Gondek, I.V. Kityk. A. Danel, Zeitschrift Naturforschung, **64a**, 632–638 (2009)
41. M. Czerwinski, J. Bieleninik, J. Napieralski, I.V. Kityk, J. Kasperczyk, R.I. Mervinskii, Europ. Polymer Journ. **33**, 1441 (1997)